ARTICLE

Resonance-Enhanced Photon Excitation Spectroscopy of the Even-Parity Autoionizing Rydberg States of Xe

Chun-yan Li, Ting-ting Wang, Jun-feng Zhen, Qun Zhang, Yang Chen*

Hefei National Laboratory for Physical Sciences at Microscale, Department of Chemical Physics, University of Science and Technology of China, Hefei 230026, China

(Dated: Received on April 24, 2008; Accepted on May 23, 2008)

Xenon atoms were produced in their metastable states $5p^5 6s[3/2]_2$ and $5p^5 6s'[1/2]_0$ in a pulsed DC discharge in a beam, and subsequently excited to the even-parity autoionizing Rydberg states $5p^5 np'[3/2]_1$,$[1/2]_1$, and $5p^5 nf'[5/2]_3$ using single photon excitation. The excitation spectra of the even-parity autoionizing resonance series from the metastable ^{129}Xe were obtained by recording the autoionized Xe^+ with time-of-flight ion detection in the photon energy range of 28000-42000 cm^{-1}. A wealth of autoionizing resonances were newly observed, from which more precise and systematic spectroscopic data of the level energies and quantum defects were derived.

Key words: Xe, Pulsed DC discharge, Resonance-enhanced photon excitation spectroscopy, Autoionizing resonance

I. INTRODUCTION

Spectroscopy on atomic highly-excited states is of great importance in many fields such as astrophysics, controlled nuclear fusion, electron correlation effects, laser isotope separation, and development of new laser systems [1,2]. The rare gas atoms (except helium) possess two relatively closely spaced ionization limits corresponding to the $^2P_{3/2}$ and $^2P_{1/2}$ states of the ionic core, with the Rydberg series converging to each of the two ionization limits. The high-lying Rydberg states of rare gas atoms, especially the autoionizing states between the two ionization limits, have been of long-standing interest to spectroscopists. Compared to other nonradiative rare gas atoms, Xe has an atomic core of the largest mass number, which implies that its Rydberg electron lies the highest in the atomic shell. Therefore the studies on the high-lying autoionizing Rydberg states of Xe may provide deeper insights into the configurations of these states and shine light on other multielectron atomic systems as well.

Since the ionization limits and the autoionizing Rydberg states of the rare gas atoms are of high energies, the spectroscopic investigations starting from their ground states usually necessitate vacuum ultraviolet (VUV) radiation, which makes their high resolution spectra hard to obtain. Promoting one of the 5p-subshell electrons of Xe to its 6s orbital yields four levels attributable to such configurations as $5p^5 6s[3/2]_{1,2}$ and $5p^5 6s'[1/2]_{0,1}$. The $5p^5 6s[3/2]_1$ and $5p^5 6s'[1/2]_1$ levels quickly decay radiatively to the ground state, while the $5p^5 6s[3/2]_2$ and $5p^5 6s'[1/2]_0$ levels are metastable with their predicted lifetimes being 149.5 s and 78.2 ms [3], respectively, and their energy positions being at 67067.54 and 76196.78 cm^{-1} relative to the ground state [4], respectively. These metastable levels facilitate access to the high-lying Rydberg levels by means of single-photon (UV) or two-photon (visible) excitation spectroscopy, a goal that is usually hard to achieve via direct VUV photon excitation starting from the ground state, partly because of the transition selection rules. More importantly, the excitation spectra can thus be obtained with a narrow-linewidth laser source, thereby ensuring high resolution.

The high-lying Rydberg states of rare gas atoms, especially the autoionizing states, have been extensively investigated [4-17]. The odd-parity autoionizing states of Xe have been studied [4-6] mainly by means of a VUV laser multiphoton excitation or a synchronization radiation of Xe from its ground state to the target states of interest. However, the studies on the even-parity autoionizing Rydberg states of Xe remain unsystematic, and the resolution of the obtained spectra is relatively low [7-17].

We present here a systematic spectroscopic study on the even-parity autoionizing Rydberg states of Xe, from which we derived more precise spectroscopic data including the level energies and the quantum defect values. This work benefited from the utilization of an optimized pulsed DC discharge for producing high number density metastable Xe* atoms in a beam. Starting from these metastable states, the high resolution excitation spectra pertinent to the autoionizing Rydberg states of Xe were readily obtained via a subsequent narrow-linewidth (<0.1 cm^{-1}) UV laser excitation.

In this work, the metastable Xe* ($5p^5 6s[3/2]_2$ and $5p^5 6s'[1/2]_0$) atoms produced in the DC discharge were excited to the even-parity autoionizing resonance se-

*Author to whom correspondence should be addressed. E-mail: yangchen@ustc.edu.cn, Tel.: +86-551-3606619, Fax: +86-551-3607084

 ©2008 Chinese Physical Society

ries $5p^5np'[3/2]_1$, $5p^5np'[1/2]_1$, and $5p^5nf'[5/2]_3$, from which the Xe atoms autoionize, giving rise to the Xe^+ detected by a time-of-flight (TOF) mass spectrometer. The excitation spectra of the autoionizing resonance series were obtained by recording the Xe^+ ion signal as a function of excitation laser wavelength.

II. EXPERIMENTS

The experimental apparatus was described in detail elsewhere [18,19]. The metastable Xe^* atoms were produced by a pulsed DC discharge of a gas mixture of 10%Xe and 90%Ar at a stagnation pressure of ~505 kPa. The DC discharge device consists of a pulsed nozzle (General Valve Co.) with an orifice diameter of 0.5 mm and a pair of parallel copper plate electrodes with a central hole whose diameter is 1 and 1.5 mm, respectively, downstream from the nozzle. Two Teflon disks were used to insulate the nozzle and the two electrodes. When the gas mixture passed through the region between the two electrodes, a pulsed high DC voltage of ~2 kV was applied to the electrodes generating a stable discharge. The supersonic atomic beam after the discharge was collimated by skimmer with a diameter of 3 mm and then entered into the observation chamber. An electric field perpendicular to the beam was applied right above the skimmer to remove the background ions out of the neutral beam. The observation chamber was maintained at a typical pressure of $\sim 1.0\times10^{-4}$ and $<1.0\times10^{-5}$ Pa, with and without operation of the beam, respectively.

A Nd:YAG (Spectra Physics, GCR-190) pumped dye laser (Lumonics, HT-500) was used as the light source. The dye laser output was frequency doubled by a second harmonic generator (Lumonics, HT-1000) and then focused perpendicularly on the metastable Xe^* beam by an f=250 mm lens. The duration of the frequency doubled laser pulse is ~8 ns, and the energy per pulse is typically ~1.0 mJ. Ions generated via autoionizing processes in the ionization zone were repelled and accelerated to the flight tube of the TOF mass spectrometer and then detected by a microchannel plate (MCP). The mass selected ion signal from the MCP detector was amplified by an amplifier (Stanford Research System, SR445) and averaged by a digital oscilloscope (Tektronix, TDS3032B) or a computer data acquisition system. A pulsed multi-channel delay generator was employed to control the relative time delays among the nozzle, the laser, and the DC discharge.

The excitation spectra were obtained by mass selectively recording the Xe^+ (m/z=124, 126, 128, 129, 130, 131, 132, 134, 136) signal as a function of the laser wavelength. No attempt was made to normalize the ion signal intensity against the laser power. The typical scanning speed of the dye laser was 1 pm/s. The laser wavelength was calibrated by a wavemeter (Coherent, WaveMaster 33-2650).

III. RESULTS AND DISCUSSION

The excited levels of the rare gas atom can be described by the $j_cl[K]_J$ coupling scheme [13,20-23], in which the orbital angular momentum l of the excited electron is weakly coupled to the total angular momentum j_c (3/2 or 1/2) of the $np5_{j_c}$ ionic core to yield the resultant quantum angular momentum K. K is then weakly coupled with the spin s of the excited electron giving the total angular momentum J. The propensity rules for electric dipole transitions in the jK-coupling scheme are generally ΔJ=0, ±1 and ΔK=0, ±1, while if ΔJ=ΔK=Δl , Δl=±1, and Δj=0 are also satisfied then the transition lines will possess higher intensity. However, since the Δj=0 rule may not be followed strictly, transitions with a change of the ionic core may also be observed.

The main interest of this work lies in the autoionizing states. Since the first adiabatic ionization potential of Xe is 97833.79 cm^{-1}, only one photon in the laser wavelength range of 235-358 nm used in the present work is required to excite the two aforementioned Xe^* metastable states to the autoionizing states of interest. The observed autoionizing states converge to the $^2P_{1/2}$ limit and decay to the $^2P_{3/2}$ limit. The following electric-dipole transitions are expected for the observed Xe transitions:

$$5s^25p^5(^2P_{3/2})6s[3/2]_2 \xrightarrow{h\nu} 5s^25p^5(^2P_{1/2})np'$$

$$\xrightarrow{h\nu} 5s^25p^5(^2P_{1/2})nf'$$

$$5s^25p^5(^2P_{1/2})6s'[1/2]_0 \xrightarrow{h\nu} 5s^25p^5(^2P_{1/2})np'$$

According to the propensity selection rules for a single-photon transition, the possible autoionizing resonance series arising from the metastable $5p^56s[3/2]_2$ level can be $5p^5(^2P_{1/2})np'[1/2]_1$,$[3/2]_1$,$[3/2]_2$ and $5p^5(^2P_{1/2})nf'[5/2]_2$,$[5/2]_3$, while the possible series arising from the $5p^56s'[1/2]_0$ metastable level can only be $5p^5(^2P_{1/2})np'[1/2]_1$,$[3/2]_1$.

Figure 1 shows schematically the energy levels and the excitation scheme for Xe, in which the relevant excitation processes from the metastable levels are denoted by two types of arrows. The solid arrows indicate the excitation processes that have been observed in our experiment, while the broken ones indicate the excitation processes that have not been observed although they are allowed transitions according to the selection rules.

Although there are many natural isotopes of Xe, the ^{129}Xe was mass selected as the target in the present study because of its highest isotopic abundance. The observed excitation spectra of ^{129}Xe in the energy range of 28000-42000 cm^{-1} are shown in Fig.2 and Fig.3. The ion signals in the two figures are in the same intensity scale, from which one can find that the spectral features in Fig.2 are much weaker than those in Fig.3.

DOI:10.1088/1674-0068/21/05/401-406 ©2008 Chinese Physical Society

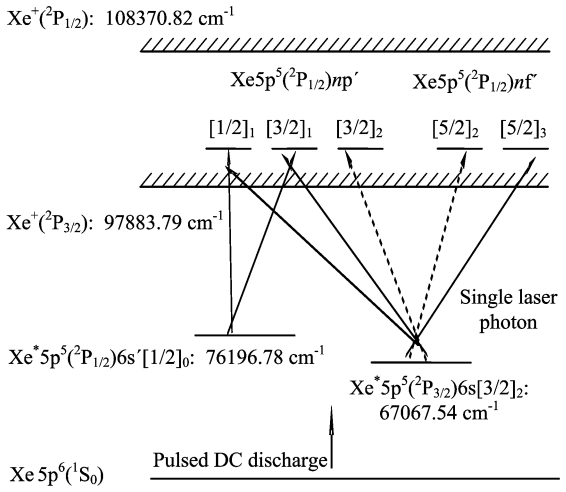

FIG. 1 Schematic diagram of the excitation processes starting from the metastable levels of xenon. The solid arrows indicate the transitions that have been observed in this experiment; the broken arrows indicate the transitions that are allowed by the selection rules but have not been observed in our experiment.

In the lower photon energy range of 28000-31500 cm^{-1} (Fig.2), two sets of spectral features were resolved. As discussed above, one can expect that the spectral intensity relating to the transition $5s^25p^5(^2P_{1/2})6s'[1/2]_0 \xrightarrow{h\nu} 5s^25p^5(^2P_{1/2})np'[3/2]_1$ should be stronger than that relating to the transition $5s^25p^5(^2P_{1/2})6s'[1/2]_0 \xrightarrow{h\nu} 5s^25p^5(^2P_{1/2})np'[1/2]_1$, and that the $5s^25p^5(^2P_{1/2})np'[1/2]_1$ levels should lie higher than the corresponding $5s^25p^5(^2P_{1/2})np'[3/2]_1$ levels, which was confirmed previously by Rundel *et al.* [12]. Therefore we assign the spectrum shown in Fig.2 as originating from the excitation transitions $5p^5(^2P_{1/2})6s'[1/2]_0 \xrightarrow{h\nu} 5p^5(^2P_{1/2})np'[3/2]_1,[1/2]_1$.

In the higher photon energy range of 30500-42000 cm^{-1} (Fig.3), there should exist three closely-spaced $5p^5np'$ series ($5p^5(^2P_{1/2})np'[1/2]_1,[3/2]_1,[3/2]_2$) excited from the $5p^56s[3/2]_2$ level, but we have only observed two of them. Following the above analysis for the lower energy range, we can assign those two series as $5p^5np'[3/2]_1$ and $5p^5np'[1/2]_1$ with some confidence. It is worth noting that only a single resonance line of the excitation from $5p^56s[3/2]_2$ was observed by Peter *et al.* who pointed out that the spectral features associated with the $5p^5np'[3/2]_2$ and $5p^5np'[1/2]_1$ resonances cannot be clearly distinguished because of a correlational shift of the $5p^5np'[1/2]_1$ resonances which yields almost the same quantum defects as the $5p^5np'[3/2]_2$ resonances [17]. On the other hand, since the lifetimes of the $5p^5np'[3/2]_2$ autoionizing resonances are relatively long, which in turn implies that the line width of the resonances should be relatively narrow, hence the line shape due to the two overlapped resonances should be mainly determined by the $5p^5np'[1/2]_1$ autoionizing resonances.

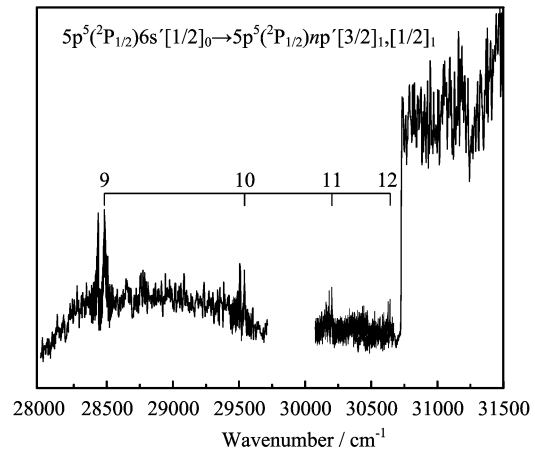

FIG. 2 Excitation spectrum arising from the metastable level $5p^56s'[1/2]_0$ of Xe in the single-photon energy range of 28000-31500 cm^{-1}.

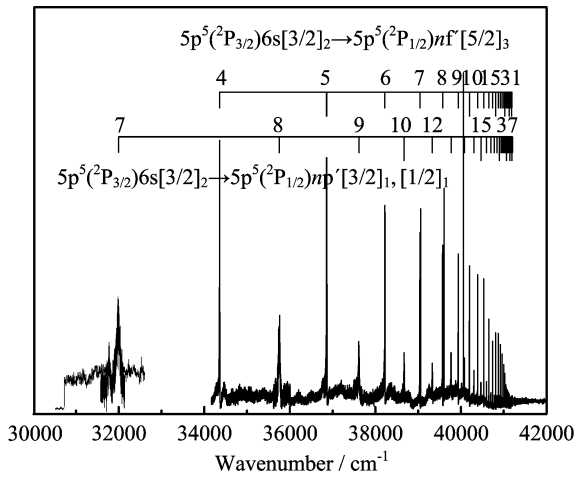

FIG. 3 Excitation spectrum arising from the metastable level $5p^56s[3/2]_2$ of Xe in the single-photon energy range of 30500-42000 cm^{-1}.

There are two possible $5p^5nf'$ series in the higher energy region shown in Fig.3. Since the $5p^5nf'[5/2]_2$ series lies very close to the $5p^5nf'[5/2]_3$ series, it is difficult to distinguish them in the spectrum. Following the $\Delta J{=}\Delta K$ rule, it is more likely that the $5p^5nf'[5/2]_3$, rather than the $5p^5nf'[5/2]_2$, accounts for the observed autoionizing resonance series excited from the $5p^56s[3/2]_2$ level.

Based on the above analyses, the observed spectral features shown in Fig.2 and Fig.3 can be identified as being due to $5p^5(^2P_{1/2})6s'[1/2]_0 \xrightarrow{h\nu} 5p^5(^2P_{1/2})np'[3/2]_1,[1/2]_1$, $5p^5(^2P_{3/2})6s[3/2]_2 \xrightarrow{h\nu} 5p^5(^2P_{1/2})np'\,[3/2]_1$, $[1/2]_1$, and $5p^5(^2P_{3/2})6s[3/2]_2 \xrightarrow{h\nu} 5p^5(^2P_{1/2})nf'\,[5/2]_3$, respectively.

The observed spectral intensity of the transition from the $6s[3/2]_2$ level to a given upper $np'[3/2]_1$ level was found to be ~10 times stronger than that of the cor-

DOI:10.1088/1674-0068/21/05/401-406 ©2008 Chinese Physical Society

TABLE I Energy term values (cm^{-1}), principal quantum numbers n, and quantum defects δ of the $5s^25p^5np'$ autoionizing states of Xe.

n	E $[1/2]_1$	δ	E $[3/2]_1$	δ	E $[1/2]_1$[a]	δ[a]	E $[3/2]_1$[a]	δ[a]
7	99066.54	3.566	98844.54	3.606	99054.6	3.568	98858.1	3.604
8	102824.54	3.552	102756.54	3.579	102817.2	3.555	102728.1	3.590
9	104682.44	3.545	104633.06	3.582	104678.9	3.548	104632.6	3.572
	104679.69*	3.547*	104632.54*	3.582*				
10	105738.64	3.543	105709.72	3.578	105736.9	3.545	105709.7	3.578
	105738.62*	3.543*	105708.64*	3.580*				
11	106399.37	3.539	106380.41	3.575	106399.3	3.539	106380.8	3.574
	106399.89*	3.538*	106380.35*	3.575*				
12	106839.15	3.536	106825.43	3.573	106837.7	3.540	106825.5	3.573
	106838.94*	3.536*	106824.94*	3.575*				
13	107144.71	3.540	107135.10	3.576	107144.6	3.540	107136.4	3.571
14	107367.80	3.540	107361.23	3.574	107369.7	3.530	107363.3	3.564
15	107535.82	3.536	107530.67	3.571	107536.6	3.531	107531.4	3.566
16	107664.25	3.538	107659.80	3.577	107662.7	3.551	107659.2	3.582
17	107764.89	3.542	107761.67	3.578	107764.4	3.548	107761.4	3.581
18	107846.30	3.536	107843.65	3.572				
19	107911.29	3.547	107909.30	3.580				
20	107965.64	3.543	107963.81	3.580				
21	108010.93	3.538	108009.59	3.570				
22	108049.11	3.531	108048.27	3.555				
23	108080.81	3.548	108079.81	3.581				
24	108108.53	3.546	108107.69	3.578				
25	108132.25	3.553	108131.24	3.598				
26	108153.13	3.548	108152.11	3.600				
27	108170.99	3.566	108169.81	3.635				
28	108187.02	3.566	108186.34	3.611				
29	108201.19	3.565						
30	108213.52	3.587						
31	108224.34	3.629						
32	108234.15	3.664						
33	108243.28	3.667						
34	108251.41	3.686						
35	108258.69	3.717						
36	108265.29	3.753						
37	108271.06	3.833						

[a] Ref.[13] (± 0.2 cm^{-1}).
* The experimental data of $6s'[1/2]_0 \xrightarrow{h\nu} np'[3/2]_1$, $[1/2]_1$ in this work.

responding transition from the $6s'[1/2]_0$ level to the same upper level. If one assumes that these two transitions have a similar probability, the observed spectral intensities may reflect the relative populations of the two metastable levels produced in our experimental conditions. Considering that the transitions $5p^56s'[1/2]_0 \xrightarrow{h\nu} 5p^5np'[3/2]_1$ should have larger transition probabilities by following the $\Delta J{=}\Delta K{=}{+}\Delta l$ rule, one can further estimate that the population ratio of the two metastable levels $6s[3/2]_2$ and $6s'[1/2]_0$ may be more than 10.

The observed energy term values of the $5p^5np'$ and $5p^5nf'$ autoionizing levels, with reference to those of the two metastable levels, are listed in Table I and Table II, respectively. The quantum defects δ are obtained by the Rydberg formula:

$$E = IP - \frac{R(^{129}\mathrm{Xe})}{(n-\delta)^2} \quad (1)$$

here E denotes the observed energy term value,

DOI:10.1088/1674-0068/21/05/401-406 ©2008 Chinese Physical Society

TABLE II Energy term values (cm^{-1}), principal quantum numbers n, and quantum defects δ of the $5s^25p^5nf'$ autoionizing states of Xe.

n	E $[5/2]_3$	δ	E $[5/2]_2$[a]
4	101425.54	0.025	101429
5	103928.90	0.030	
6	105289.46	0.032	
7	106109.47	0.034	106112
8	106640.34	0.037	106642
9	107004.78	0.037	107008
10	107265.18	0.037	107267
11	107457.74	0.037	107459
12	107603.62	0.040	107605
13	107716.89	0.046	108371
14	107807.05	0.048	
15	107880.18	0.045	
16	107939.62	0.047	
17	107988.86	0.050	
18	108030.68	0.038	
19	108065.37	0.046	
20	108094.92	0.057	
21	108120.47	0.064	
22	108142.68	0.068	
23	108162.06	0.073	
24	108179.09	0.076	
25	108194.44	0.057	
26	108207.78	0.056	
27	108219.44	0.076	
28	108230.26	0.059	
29	108240.03	0.034	
30	108248.70	0.024	
31	108255.98	0.088	

[a] Ref.[10] (± 2 cm^{-1}).

$R(^{129}Xe)$=109736.856 cm^{-1} the Rydberg constant of ^{129}Xe, n the principal quantum number, δ the quantum defect, and IP the ionization potential. $IP(^2P_{3/2})$=97833.79 cm^{-1} when the ion is in the j_c=3/2 state, and $IP(^2P_{1/2})$=108370.82 cm^{-1} when the ion is in the j_c=1/2 state. The derived quantum defect values are also listed in Table I and Table II.

The quantum defects of all resonance series were found to increase with increasing the principal quantum number n, except for some irregularity [24]. Since the quantum defect reflects how much the average potential experienced by the Rydberg electron deviates from a pure Coulombic point charge interaction, the experimental data indicate that the Rydberg electron penetrates closer to the nuclei with higher quantum number. Because the observed autoionizing resonances occur in the $^2P_{3/2}$ continuum which lies between the two ionization limits, the perturbation arising from interactions among the resonance series having the same parity and J, and the perturbation arising from interactions between the resonance series and the $^2P_{3/2}$ continuum, are rather complex. Such perturbations should influence the Rydberg electron of Xe, which manifests itself in the variation of the quantum defects. The width of the spectral peak reflects the lifetime of the corresponding resonance. The experimental results show that, as the principal quantum number n increases, the quantum defects of a given series increase, whereas the widths of the autoionizing resonance peaks corresponding to the given series decrease. This is anticipated simply because the interactions between the resonance series and the $^2P_{3/2}$ continuum become greater when approaching the second ionization limit.

IV. CONCLUSION

We carried out an experimental study on the autoionizing $5p^5np'$ and $5p^5nf'$ resonance series of xenon by using pulsed DC discharge together with a single UV photon excitation followed by a time-of-flight ion detection. We have presented an abundance of new data regarding the Rydberg autoionizing levels of xenon excited from the two metastable levels $5p^56s[3/2]_2$ and $5p^56s'[1/2]_0$. From these newly observed autoionizing resonances of xenon, we have obtained more systematic information on the level energies and quantum defects of xenon.

V. ACKNOWLEDGMENTS

This work was supported by the National Natural Science Foundation of China (No.20673107), the Chinese National Key Basic Research Special Foundation (No.2007CB815203), and the Chinese Academy of Science (No.KJCX2-SW-H08).

[1] K. Z. Xu, *Advanced Atomic and Molecular Physics*, Beijing: Science Press, 4 (2000).
[2] T. X. Lu and Y. Q. Lu, *Principles and Applications of Laser Spectroscopic Techniques*, Hefei: University of Science and Technology of China Press, 368 (1999).
[3] N. E. Small-Warren and L. Y. Chow Chiu, Phy. Rev. A **11**, 1777 (1975).
[4] M. Hanif, M. Aslam, R. Ali, S. A. Bhatti, M. A. Baig, D. Klar, M. W. Ruf, I. D. Petrov, V. L. Sukhorukov, and H. Hotop, J. Phys. B: At. Mol. Opt. Phys. **37**, 1987 (2004).
[5] J. Z. Wu, S. B. Whitfield, C. D. Caldwell, M. O. Krause, P. van der Meulen, and A. Fahlman, Phys. Rev. A **42**, 1350 (1990).
[6] S. M. Koeckhoven, W. J. Burma, and C. A. de lange, Phys. Rev. A **49**, 3322 (1994).

DOI:10.1088/1674-0068/21/05/401-406 ©2008 Chinese Physical Society

[7] M. Thekaekara and G. H. Dieke, Phys. Rev. **109**, 2029 (1958).
[8] P. R. Blazewicz, J. A. D. Stockdale, J. C. Miller, T. Efthimipoulos, and C. Fotakis, Phys. Rev. A **35**, 1092 (1987).
[9] S. M. Koeckhoven, W. J. Burma, and C. A. de lange, Phys. Rev. A **51**, 1097 (1995).
[10] M. Gisselbrecht, A. Marquette, and M. Meyer, J. Phys. B: At. Mol. Opt. Phys. **31**, L977 (1998).
[11] M. Meyer, M. Gisselbrecht, A. Marquette, C. Delisle, M. Larzilliere, I. D. Petrov, N. V. Demekhina, and V. L. Sukhorukov, J. Phys. B: At. Mol. Opt. Phys. **38**, 285 (2005).
[12] R. D. Rundel, F. B. Dunning, H. C. Goldwire Jr., and R. F. Stebbing, J. Opt. Soc. Am. **65**, 628 (1975).
[13] R. D. Knight and L. G. Wang, J. Opt. Soc. Am. B **3**, 1673 (1986).
[14] R. Kau, D. Klar, S. Schohl, S. Baier, and H. Hotop, Z. Phys. D **36**, 23 (1996).
[15] J. P. Grandin and X. Husson, J. Phys. B: At. Mol. Opt. Phys. **14**, 433 (1981).
[16] M. Hanif, M. Aslam, M. Riaz, S. A. Bhatti, and M. A. Baig, J. Phys. B: At. Mol. Opt. Phys. **38**, S65 (2005).
[17] T. Peter, T. Halfmann, U. Even, A.Wunnenberg, I. D. Petrov, V. L. Sukhorukov, and H. Hoptop, J. Phys. B: At. Mol. Opt. Phys. **38**, S51 (2005).
[18] T. T. Wang, C. Y. Li, X. F. Zheng, L. S. Pei, and Y. Chen, Chin. Sci. Bull. **52**, 596 (2006).
[19] T. T. Wang, X. F. Zheng, C. Y. Li, and Y. Chen, Chem. Phys. Lett. **425**, 185 (2006).
[20] G. Racah, Phys. Rev. **62**, 438 (1942).
[21] I. I. Sobelman, *Atomic Spectra and Radiative Transitions*, Heidelberg: Springer-Verlag, 173 (1979).
[22] R. D. Cowan, *The Theory of Atomic Structure and Spectra*, California: University of California Press, 485 (1981).
[23] U. Fano, Phys. Rev. **124**, 1866 (1961).
[24] F. B. Dunning and R. F. Stebbing, Phys. Rev. A **9**, 2378 (1974).

DOI:10.1088/1674-0068/21/05/401-406 ©2008 Chinese Physical Society